Journal of Solid State Chemistry **154,** 301–306 (2000)
doi:10.1006/jssc.2000.8853, available online at http://www.idealibrary.com on IDEAL®

Microanalysis of Light Elements by Means of a Nuclear Microprobe: Application to Boron Compounds

P. Berger,* E. Tominez,† C. Godart,† E. Alleno,† L. Daudin,* and J-P. Gallien*

*Laboratoire Pierre SÜE (CEA/CNRS), Centre d'Etudes Nucléaires de SACLAY 91191, Gif sur Yvette Cedex, France; and †L.C.M.T.R., UPR209, C.N.R.S., 2-8 rue Henri Dunant, 94320 Thiais, France

Received October 19, 1999; in revised form May 19, 2000; accepted June 1, 2000

The nuclear microanalysis is an elemental analysis technique based on the use of the atomic and nuclear interactions of a light ion microbeam with the sample to be analyzed. Both light particles and photons (X, γ) are detected. The determination of the local stoichiometry of boron-based compounds is possible with the use of nuclear reactions. Boron and carbon mapping of YPd-based borocarbides is presented. Additional possibilities of in-depth carbon profiling are also reported. © 2000 Academic Press

INTRODUCTION

The synthesis and the understanding of the properties of nonorganic compounds have always been elemental analysis consuming as well for the trace than for the major elements. In this latter case, the nature of the elements is already known but the stoichiometry of the synthesized phases is not accurately determined, either because the mass balance is not equilibrated (mass losses during the synthesis process) or because the sample contains several phases.

Most methods of direct elemental characterization on bulk samples, without any dissolution procedures, probe the electronic properties of the constitutive elements of the sample. For elements with medium or high atomic numbers, when core electrons are involved, the signals coming from the interaction of the probe with the sample have well defined energies. On the other hand, the energy levels of light elements depend on the chemical bonding. For a given element, the shape and the intensity of the emitted signals may vary according to the nature of the compound. Quantitative analysis requires then the use of numerous standards with compositions as close as possible to that of the sample to be analyzed.

Alternative techniques with a lower dependence on standards are then especially attractive for light elements. Nuclear microanalysis, based on the interaction of an ion microbeam with the sample, meets this demand since it probes the nuclear properties of the elements, independently of the chemical bonding. Nuclear microanalysis is a branch of ion beam analysis (IBA). Its specificity comes from the reduced size of the beam, within the micrometer size, which enables investigations on the lateral heterogeneities of composition at the micrometer scale.

The aim of this paper is to give an overview of the main features of nuclear microanalysis on light elements, but with a special emphasis on the measurement of boron and on stoichiometry determinations on boron-based compounds.

BASIC INTERACTIONS

The nuclear microprobe focuses a few-MeV light ion microbeam (mostly ^{1}H, ^{2}H, ^{3}He, and ^{4}He) on the sample. The analytical techniques are based on the detection of emitted particles and photons (X and γ). The methods of detection are numerous, but they all derive from basic atomic and nuclear interactions.

In the MeV range, when penetrating through matter, most of the ions follow straight lines, gradually losing their energy by electronic interaction. The rate of energy loss, $\mathrm{d}E/\mathrm{d}x$, measured in units of MeV ($\mathrm{g\,cm^{-2}}$), can be calculated from the weighted mean of the $\mathrm{d}E/\mathrm{d}x$ values for the constituent elements with only very slight dependence on the chemical bonding (Bragg rule) (1).

Along the track of the ion, the atoms are excited or ionized and the relaxation of inner-shell vacancies leads to the emission of X-rays in the 1- to 30-keV range, characteristic of the elements (2). The related analytical technique is named PIXE (particle-induced X-ray emission) and is suitable for medium to heavy elements ($Z > 10$). Compared to the electrons, the ions induce much smaller bremsstrahlung radiation background, because of the higher mass of the ions. Compared to the electron probe, the elemental sensitivity of PIXE is enhanced by a factor 10–100 (3, 4). The PIXE is often used at the nuclear microprobe in combination with other analytical techniques detailed below.

The nuclear interactions are specific of the nuclear microanalysis. The scattering of the ions of the beam by the coulomb repulsion of the nuclei of the sample is the basis of

0022-4596/00 $35.00

a family of techniques, among which Rutherford backscattering (RBS), because of its accuracy and simplicity (5), is the most used. Backscattered ions are collected and their energy spectrum is composed of as many superimposed steps as elements present in the sample.

A light ion scattered at a backward angle loses more of its energy in a collision on a light nucleus than it would after a collision on an heavy one. The energy position of the steps allows then the identification of the mass of the nuclei of the target. For thick targets, because of the energy loss of the ions entering and leaving the sample, the energy spectrum is continuous and depth information may be extracted from the energy shift from the surface. The depth resolution depends on the energy loss, of the ions, the higher the loss the higher the resolution (currently a few 10 nm with ^{4}He). As the energy loss and the mass resolution (separation between neighboring elements of the target) increases with the mass of the incoming ion, RBS is better performed with ^{3}He and ^{4}He than with ^{1}H and ^{2}H. Figure 1 shows an example of a RBS spectrum induced by 3 MeV ^{3}He on a $HoNi_2B_2C$ sample. As the cross sections of RBS are proportional to the square of the atomic number of the elements, the nickel step appears to be smaller than the holmium step, although its atomic concentration is twice as high.

As a consequence of the cross sections' dependence on the atomic number, the sensitivity of RBS is low for light elements. Resonances and enhanced elastic scattering may occur for some values of the energy of the incident ions (particle enhanced scattering analysis (PESA)), depending on their nature and related to the nuclear structure of light elements from He to Si (6–8). This possibility will not be discussed here.

Nuclear reaction analysis (NRA) is by far the most versatile method for measurement of light elements. This technique relies on the detection of charged particles, neutrons, or γ-rays emitted in nuclear reactions. The inelastic collision between the ions of the probe and the light nuclei of the target lead to the formation of new nuclei, usually with the emission of particles differing from the incident ions. As most of the nuclear reactions are exoenergetic, the emitted particles carry higher energies than the incident ions. These particles may be then easily distinguished from the backscattered ones.

To induce a nuclear reaction, the incident ion must have enough energy to overcome the coulomb barrier of the target nucleus. The higher the atomic number, the higher the barrier is. Although the energy of the ions of the microprobe is limited to a few MeV, light elements from hydrogen to sulfur may be analyzed. As the occurrence of a nuclear reaction depends on the nuclear properties of the involved nuclei, the nuclear reaction analysis is isotopically selective (6, 7, 9, 10). Table 1 reports a short list of nuclear reactions for analytical purpose.

The newly formed nuclei may be left in an excited state whose relaxation leads to the emission of characteristic γ-rays, ranging from hundreds of keV to several MeV. Particle-induced γ-ray emission (PIGE) is the analytical technique based on their spectroscopy (6, 7, 11). The excitation energy of the remaining nuclei limits the energy of the produced particles. Their energy spectrum presents several groups, corresponding to the different energy levels of the produced nuclei. As an example, Figs. 2 and 3 show spectra induced, respectively, by 3.0 MeV ^{3}He and 1.4 ^{2}H on pure boron and carbon samples. The detector is covered with a mylar absorber foil to avoid the detection of the backscattered incident particles. For each element, several groups

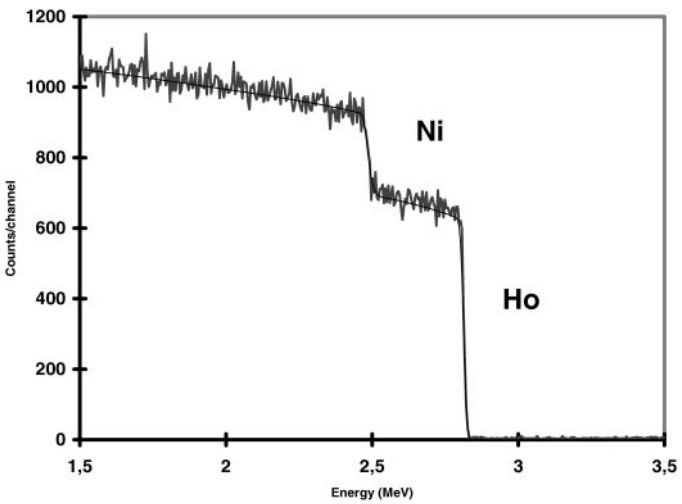

FIG. 1. RBS spectrum induced by 3.0 MeV ^{3}He on an $HoNi_2B_2C$ sample.

TABLE 1
List of a Few Useful Nuclear Reactions

Isotope	Nuclear reaction	Detected	Energy of the particle
^{6}Li	^{6}Li(d,α)^{4}He	α	9.5(1)
^{7}Li	^{7}Li(p,α)^{4}He	α	8.0(1)
^{9}Be	^{9}Be(d,p)^{10}Be	p	5.0(1)
^{10}B	^{10}B(d,p)^{11}B	p	8.8(2)
	^{10}B(d,α)^{8}Be	α	11.0(2)
	^{10}B(^{3}He,p)^{12}C	p	18.8(3)
^{11}B	^{11}B(d,p)^{12}B	p	1.8(2)
	^{11}B(d,α)^{9}Be	α	5.3(2)
	^{11}B(p,α)^{8}Be	α	6.1(1)
	^{11}B(^{3}He,p)^{13}C	p	13.3(3)
^{12}C	^{12}C(d,p)^{13}C	p	3.6(1)
	^{12}C(^{3}He,p)^{14}N	p	6.0(3)
^{14}N	^{14}N(d,p)^{15}N	p	8.6(2)
^{16}O	^{16}O(d,p)^{17}O	p	2.4(1)
^{18}O	^{18}O(p,α)^{15}N	α	4.1(1)
^{19}F	^{19}F(p,α)^{16}O	α	7.4(1)

Note. Detection at 135°: (1) 1.5 MeV deuterons; (2) 2.0 MeV protons or deuterons; (3) 3.0 MeV ^{3}He.

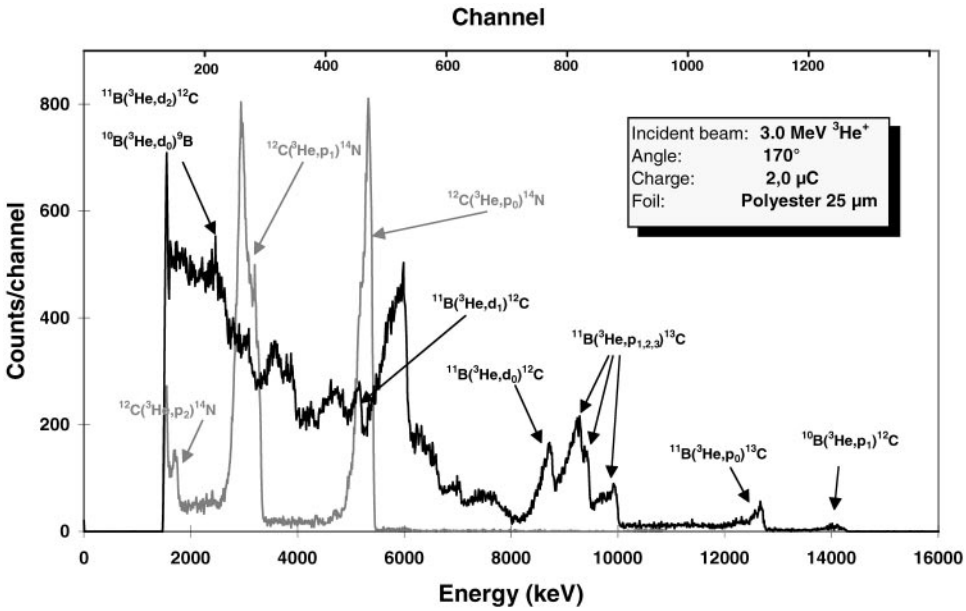

FIG. 2. NRA spectrum induced by 3.0 MeV ^{3}He on pure boron and carbon samples, respectively.

are observed, for instance $^{10}B(d, p_i)^{11}B$ $(i = 0 \rightarrow 7)$, each group corresponding respectively to the excited states of the ^{11}B. Note that for deuterons, the respective contribution of the ^{10}B starts from much higher energies than that of the ^{11}B, because the reactions induced by ^2H on the ^{10}B are more energetic than those on ^{11}B.

Like for the elastic scattering, the energy spectrum of the emitted particles may be converted into a depth profile, provided that the different groups do not overlap. Contrary to the RBS for which the scattering cross-sections can be easily calculated, the evolutions of the cross sections of the nuclear reactions with the energy and with the angle of detection have to be experimentally measured. As the incoming ion loses its energy as it penetrates through the sample, the yield of the nuclear reaction varies with the depth. The shape of the energy spectrum of the emitted particles reflects then the evolutions of the cross sections with the energy of the incident ion. Figure 3 shows an example with the $^{12}C(d, p)^{13}C$ nuclear reaction. Since the sample is a pure phase (i.e., an homogeneous carbon distribution), the shape of the proton group reflects the cross-section evolution with the energy of the deuterons.

For a sample with a nonhomogeneous carbon depth distribution, the carbon concentration depth profile may be

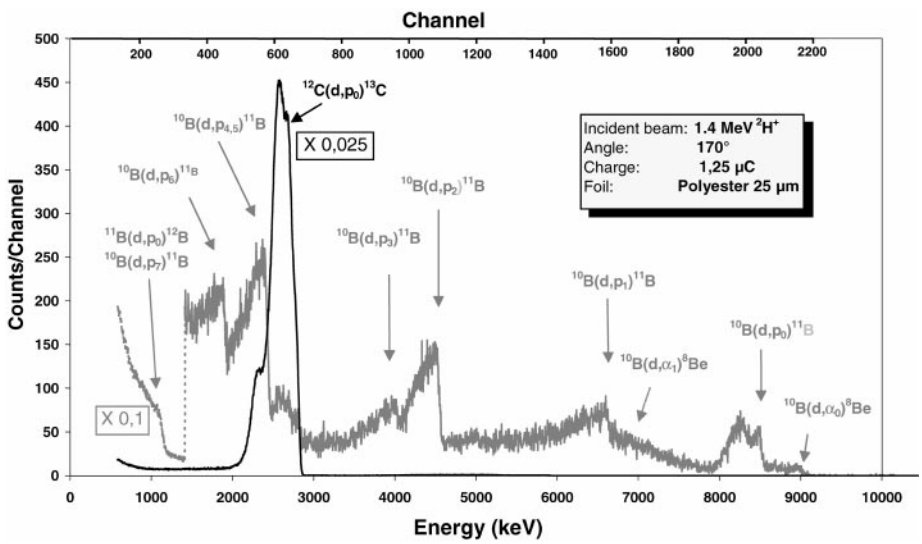

FIG. 3. NRA spectrum induced by 1.4 MeV ^{2}H on pure boron and carbon samples, respectively.

extracted from the spectrum. Compared to the RBS, the depth resolution is generally lower (≥ 50 nm) because the energy loss of the particles is lower (higher energy and lower mass of the produced particles). An increase of the depth resolution (5–10 nm) may be obtained for a few elements by the use of resonances which correspond to a strong increase of the cross sections for a very narrow energy window, practically on the order of a few keV (12). This possibility is not discussed here.

BORON COMPOUNDS CHARACTERIZATION

The local characterization of boron compounds requires the measurement of all the elements since the boron stoichiometry can be deduced from the yield of the nuclear reactions only if the analyzed depth is determined.

The estimation of the analyzed thickness is based on the computation of the range of the incident ions, depending on the sample composition. The use of nuclear reaction analysis for the measurement of light elements must be then coupled to the measurement of the induced X-rays (PIXE) or of the backscattered particles (RBS) to obtain the cation stoichiometry. This is a crucial point for the microprobe measurements when the lateral heterogeneities of composition concern all the elements.

The methods of measuring boron content are numerous (13, 14), but the selection of the best one depends on the energy range of the accelerator (minimum and maximum energy of the particles) and of the other light elements to be measured (sufficient sensitivity for all the measured elements and lack of interferences).

A typical example is given by the characterization of yttrium/palladium-based borocarbides, for which both boron and carbon contents have to be determined (15–17). As-cast samples of nominal composition $YPd_5B_3C_{0.3}$ exhibit superconducting and magnetic properties, but the phase responsible for this behavior was not unambiguously identified. The SEM micrography of the microstructure reveals at least six phases, especially a few micrometer-wide needles. These may represent the superconducting phase since the needles disappear after annealing, while the sample no longer exhibits superconductivity.

The characterization of these needles and of some of the other phases has been done with the nuclear microprobe using either a ^{3}He or a ^{2}H microbeam. Although the nuclear reactions induced on boron by ^{3}He and ^{2}H are similar, the sensitivity on the carbon determination with ^{2}H is greatly enhanced, which favors the stoichiometric determination of low carbon phases. However, the mass separation of yttrium and palladium on the RBS spectra is much better with ^{3}He than with ^{2}H. One can note that the cross sections of the different nuclear reactions involved are not all known. The simulation *a priori* of the spectra is then not possible.

The NRA spectrum of a borocarbide is more or less a combination of the spectra obtained, respectively, on pure carbon and on pure boron (Fig. 4 shows a spectrum measured on a superconducting needle). The standardization does not require numerous reference samples. Measurements on pure phases would be sufficient, but the accuracy has been checked with samples of known stoichiometry (YB_2C_2 and HoB_2C_2). The carbon versus boron content is estimated by comparing the yield of two energy windows in the same NRA spectrum, one related to the boron alone and the other to a mixed response of boron and carbon. The heavy elements' stoichiometry being known (i.e., Y versus Pd ratio determined from PIXE, RBS, or, in some cases, the

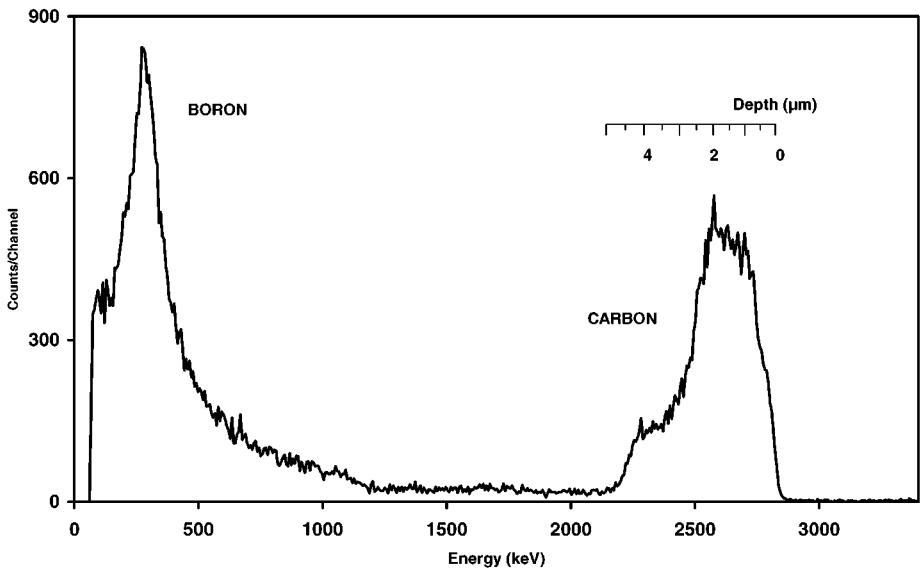

FIG. 4. NRA spectrum induced by 1.4 MeV ^{2}H on a superconducting needle, YPd_2B_2C.

electron probe measurements) and the experimental yield on the light elements for a given number of incident ions being measured (for instance, the measurement of the quantity of boron within the analyzed thickness (number of B atoms/cm^2)), a computation of the range of the particles as a function of the elemental composition makes it possible to find the full stoichiometry. The composition of the phases found in the Y–Pd–B–C samples is reported in the papers of Godart *et al.* (15–17).

MICROSTRUCTURE MAPPING

The scanning of the ion microbeam is an efficient way of investigating multiphase samples, especially when the image of the surface (optical or electronic) presents low contrast. Instead of the usual stationary position on the sample, the beam is scanned across the interest zone and the spectra of the different interactions (NRA, PIXE, RBS, PIGE, etc.) are recorded as a function of the position of the beam. By selecting an appropriate energy window in a given spectrum, the corresponding map reveals the fluctuations of concentration. Figures 5a and 5b show the maps of the intensiti es of the nuclear reactions induced, respectively, on carbon and on boron by a microbeam of 1.4 MeV deuterons on an as-cast YPdBC sample (surface covered $130 \times 80\ \mu m^2$ with a beam size of $3 \times 2\ \mu m^2$). The superconducting needles, a carbon-rich phase, found to be YPd_2B_2C, compared to the matrix, a low carbon phase, $YPd_{7.1}B_{4.2}$, are clearly evidenced. The precision of the stoichiometric determination is now limited to 3–4% by the counting statistics of the high-energy part of the boron spectra. Better precision might be achieved (1–2%) with the use of the low-energy part of the spectra (higher counting statistics, especially suitable for mapping), but the origin of observed fluctuations of the background is not yet well understood.

As the carbon NRA spectrum is depth resolved (here ≈ 250 nm, cf. depth scale on Fig. 4), the shape and the thickness of the needles might be reconstructed. Buried needles may also be evidenced. On the carbon map of Fig. 5a, near the main needle, a small one appears on the lower left. By selecting an energy window in the spectrum restricted to the shallow depth carbon, this small needle does no longer appears because it is buried at least 500 nm under the surface (cf. Fig. 6).

Also, the depth resolution on the carbon profile makes it possible to check for surface carbon contamination. The carbon concentration determination might be determined without taking into account the surface carbon.

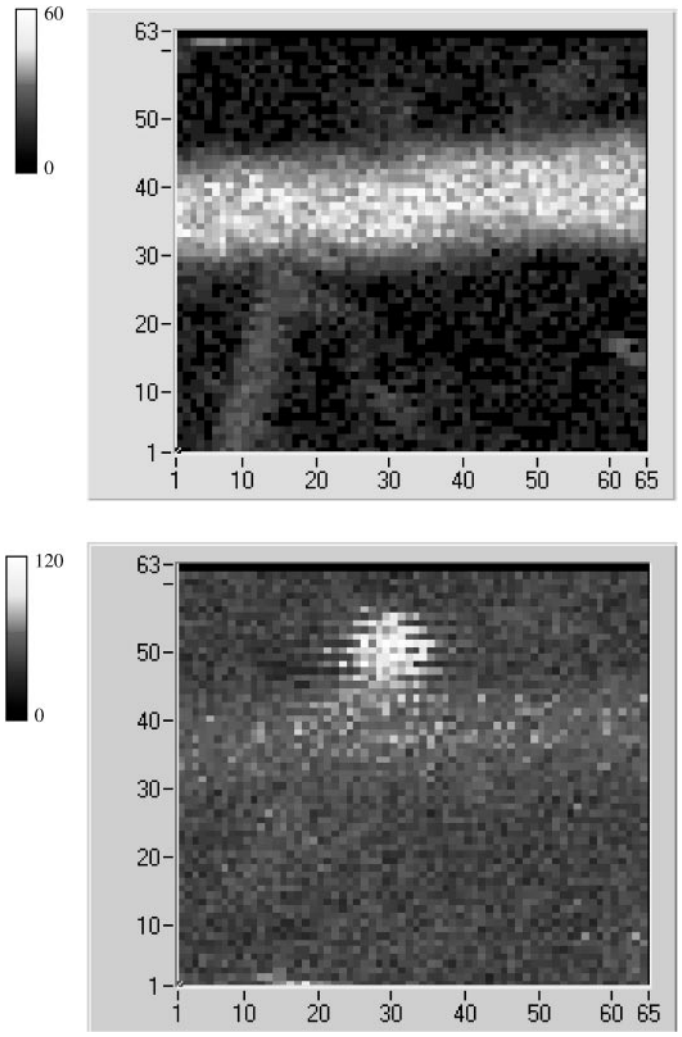

FIG. 5. (a) Carbon map induced by a 1.4-MeV ^{2}H microbeam on a sample of nominal composition $YPd_5B_3C_{0.3}$ (X step, 2 μm; Y step, 1.25 μm). (b) Boron map induced by a 1.4-MeV ^{2}H microbeam on a sample of nominal composition $YPd_5B_3C_{0.3}$ (X step, 2 μm; Y step, 1.25 μm).

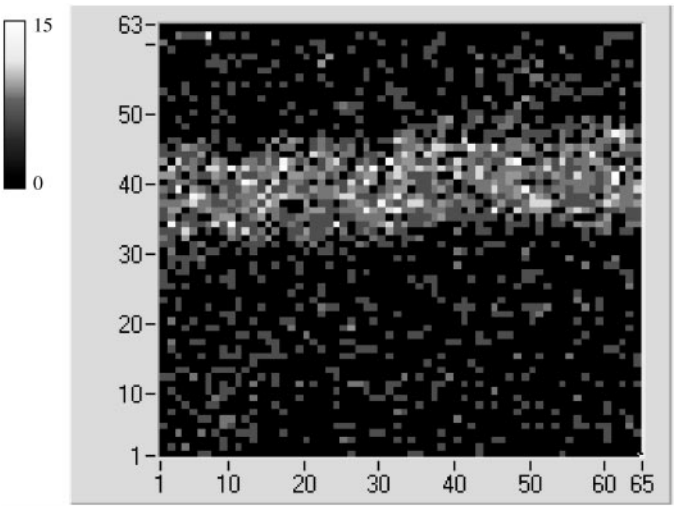

FIG. 6. Carbon map restricted to shallow depth (X step, 2 μm; Y step, 1.25 μm).

CONCLUSION

Nuclear microanalysis is a powerful tool for investigating the concentration of light elements in multiphase samples. In the case of boron, the stoichiometry of boron based compounds may be determined with a good accuracy, provided that the sample is homogeneous in the analyzed zone (a few μm^3).

Because of the limited number of laboratories operating MeV ion microbeams, ion beam-based microanalytical techniques are not extensively used. In order to improve the access to these techniques, the nuclear microprobe of the Pierre SÜE laboratory works as a national facility, open to the scientific community.

REFERENCES

1. N. N. Anderson and J. F. Ziegler, "Stopping Powers and Ranges in All Elements." Pergamon Press, NY, 1977.
2. F. Folkmann, *in* "Materials Characterization Using Ion Beams" (J. P. Thomas and A. Cachard Eds.). Plenum, 1978. New York, 239.
3. S. AE. Johansson and J. L. Campbell, "PIXE, a Novel Technique for Elemental Analysis." John Wiley, Chichester, 1988.
4. J. L. Campbell, W. J. Teesdale, and J. A. Maxwell, *Nucl. Inst. Methods B* **56/57,** 694 (1991).
5. W. K. Chu, J. W. Mayer, and M. A. Nicolet, "Backscattering Spectrometry." Academic press, NY, 1978.
6. J. W. Mayer and E. Rimini, "Ion Beam Handbook for Materials Analysis." Academic Press, NY, 1977.
7. J. R. Bird and J. S. Williams, "Ion Beam Handbook for Materials Analysis." Academic Press, Sidney, 1990.
8. J. R. Tessmer and M. Nastasi, "Handbook of Modern ion beam Materials Analysis." Materials research society, Pittsburg, 1995.
9. G. Deconninck, "Introduction to Radioanalytical Physics." Elsevier, Amsterdam, 1978.
10. G. Demortier, *Nucl. Instr. Methods B* **104,** 244 (1995).
11. B. Borderie, *Nucl. Instr. Methods* **175,** 465 (1980).
12. Vizkelety *et al.*, *Surf. Interface Anal.* **20,** 309 (1993).
13. A. E. Pillay and M. Peisach, *Nucl. Instr. Methods B* **66** (1992) 226.
14. N. Moncoffre *et al.*, *Nucl. Instr. Methods B* **45,** 81 (1990).
15. C. Godart *et al.*, *Phys. Rev. B* **51**(1), 489 (1995).
16. E. Tominez, P. Berger, *et al.*, *J. Alloys compounds* **275–277,** 123 (1998).
17. E. Tominez, E. Alleno, P. Berger, M. Bohn, C. Mazumdar, C. Godart, *J. Solid State Chem.* **154,** 114 (2000).